Phase behavior of lattice associating binary mixtures: A Monte Carlo study

A. Patrykiejew,[1] L. Salamacha,[1] S. Sokołowski,[1] H. Dominguez,[2] and O. Pizio[2]
[1]*Faculty of Chemistry, MCS University, 20031 Lublin, Poland*
[2]*Instituto de Quimica, UNAM, Mexico City, Mexico*
(Received 18 November 2002; published 14 March 2003)

The lattice gas model is used to study effects of molecular association on the phase behavior of binary symmetric mixtures, in which only dimers consisting of different particles can form. It is demonstrated that the increase of the association energy leads to qualitative changes of the phase diagrams. In particular, the demixing transition is observed only for sufficiently low association energy. That demixing transition can be either first order or continuous. For sufficiently high energy of association the condensed phase shows a very well ordered structure even at high temperatures.

DOI: 10.1103/PhysRevE.67.031202 PACS number(s): 61.20.Qg, 61.20.Ja, 64.70.Fx

I. INTRODUCTION

The phase behavior of associating binary mixtures is an area of intense activity [1–16]. The interest in such systems mainly stems from a desire for a better understanding of fluid mixtures with hydrogen bonds [1], such as water and various solutions. The most pronounced effect of molecular association in mixtures is the appearance of the so-called close loop liquid-liquid immiscibility and the existence of lower and upper critical solution temperatures [1,7]. In general, these reentrant phenomena can be explained as resulting from competing effects due to molecular interactions, including the formation of associates, and entropic effects. At sufficiently low temperatures, below the lower critical solution point, the entropic effects are overcome by the large contributions to the free energy resulting from the formation of associates. Under such conditions, the mixture may have a well defined ordered structure, which involves both components. As the temperature increases, the association is gradually inhibited and when the interaction between unlike particles is considerably weaker than the interaction between like particles, the mixture may separate into two phases. A further increase of temperature, above the upper critical solution point, causes entropic effects to become dominating over the enthalpic contribution and hence induces miscibility. The above remarks apply to already condensed liquid systems.

The problem of gas-liquid condensation in associating binary mixtures becomes much more difficult and is also less understood. It is enough to mention that the phase behavior of a simple (nonassociating) binary mixture is still far from being solved. As Wilding, Schmid, and Nielaba [17] have remarked: "... it is not well understood (even at the mean-field level) precisely which microscopic features are responsible for yielding a given [phase diagram] topology." A common feature of such systems is the presence of a line of continuous transitions (the so-called λ line [18]) between mixed and demixed phases. That continuous transition occurs at sufficiently high temperatures and, upon the decrease of temperature, the λ line terminates at the tricritical or at the critical end point. At lower temperatures, the system undergoes the first-order condensation transition from a mixed vapor to a demixed liquid phase. Depending on the microscopic parameters representing interactions in the system, the condensation transition may terminate at the ordinary critical point, or at the tricritical point, where the λ line begins. In the former case, the system may also exhibit the presence of the triple point, in which mixed vapor coexists with mixed as well as with demixed liquid. Thus, above the triple point another first-order transition between mixed and demixed liquid phases occurs. This transition terminates at the tricritical point, which is the onset of the λ line. The λ line may also start at a certain point at a liquid side of the vapor-liquid coexistence below critical point (at the liquid side) at the critical end point. The above presented scenarios may, or may not, hold in the case when additional, associating, interactions are present.

The majority of theoretical [4,7–9,14,15,19–23] and computer simulation [10,13,19,24] studies of associating fluids have concentrated on the behavior of liquid phases aiming at a better understanding of the mechanism leading to the appearance of the lower and upper critical solution temperatures. In particular, computer simulation methods are well known tools allowing for highly accurate determination of the phase behavior of physical systems [25–27] and have already been used to study lattice [10] and continuous [13] models of associating fluids.

In this paper we report on the results of grand canonical Monte Carlo study of lattice associating symmetric binary mixtures consisting of *A* and *B* particles and characterized by the same strength of interaction between the pairs of like particles, and by varying strength of the association interaction. Our main goal has been to determine how the association influences the phase diagram topology, and we concentrate only on the condensation of a dilute gas phase into a liquid phase. The model we use is similar to that considered by Kotelyanskii *et al.* [10], but they studied rather special case of a fully occupied lattice that permits to study only transitions between condensed phases.

The paper is organized as follows. Section II is devoted to the presentation of the model, its ground state properties and describes the Monte Carlo method. The following Sec. III presents the results of our calculations. The paper concludes in Sec. IV, which summarizes our findings.

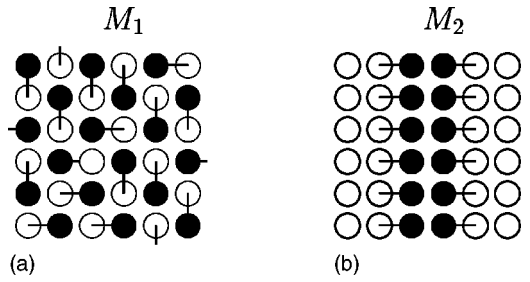

FIG. 1. Schematic two-dimensional picture of the ordered mixed structures (a) M_1 and (b) M_2.

II. THE MODEL AND MONTE CARLO METHOD

As already has been mentioned, we consider a lattice gas model of a binary mixture of the components A and B. Each particle occupies a single site of a cubic lattice and interacts only with the first nearest neighbor particle. The energies of interaction between different pairs (AA, BB and AB) are denoted by u_{AA}, u_{BB}, and u_{AB}. Besides, each particle $A(B)$ has one acceptor (donor) that can participate in the formation of a dimer. Since the particles are structureless, the donors and acceptors do not have any prespecified locations. The association energy u_{as} is finite and hence the dimers are allowed to dissociate.

With the above assumptions, the Hamiltonian of the model can be written as

$$\mathcal{H}=u_{AA}\sum_{\langle ij\rangle} n_i^A n_j^A+u_{BB}\sum_{\langle ij\rangle} n_i^B n_j^B+u_{AB}\sum_{\langle ij\rangle} n_i^A n_j^B+u_{\mathrm{as}}\sum_{\langle ij\rangle} \gamma_{ij} - \mu_A\sum_i n_i^A-\mu_B\sum_i n_i^B, \tag{1}$$

where n_i^K is the occupation variable equal to unity when the ith site is occupied by a particle of component K ($K=A$ or B), γ_{ij} equal to 1 when the both particles on sites i and j form a bond and equal to 0 otherwise, μ_A and μ_B are the chemical potentials of both components. The first four sums run over all distinct pairs of nearest neighbors, while the last two sums are taken over all sites.

At the ground state, the model predicts the formation of the following ordered phases: the two condensed pure phases of A and B and the two different mixed phases M_1 and M_2, in which half of the sites is occupied by one component and other half by the second component, with the structure schematically shown in Fig. 1. The phase M_1 is characterized by a random orientation of ''bonds'' resulting from the association, while in the phase M_2 these bonds assume mutually parallel orientation. Of course, one has to include the gas phase (of zero density at $T=0$) as well. Since the structure of the all possible phases at the ground state is known, one can readily determine the conditions of stability for all of them and to calculate the phase diagrams at $T=0$. Before we present the ground state phase diagrams for the above model, it is worth to mention that only one of the mixed phases M_1 and M_2 can appear for any given set of interaction parameters and the condition, which determines which of them is stable, does not depend on the association energy. The phase M_1 is more stable, than the phase M_2 whenever

$$2u_{AB}<u_{AA}+u_{BB}, \tag{2}$$

while the phase M_2 occurs when the above condition is not satisfied, but only for appropriately chosen energy of association (see discussion below).

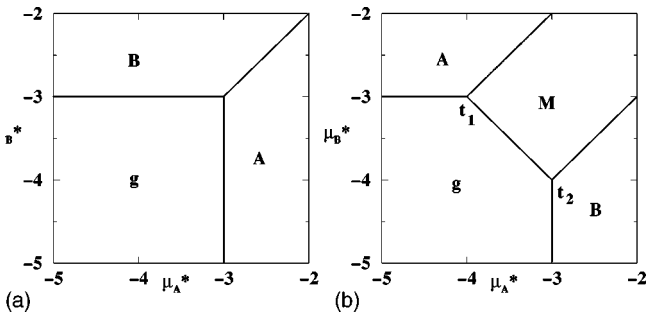

FIG. 2. The two possible ground state phase diagrams for the model used in this work. (a) shows the phase diagram for systems which do not form mixed condensed phases, while (b) corresponds to the systems which may form either the M_1 or M_2 condensed phase (labeled by M in the figure). The triple points are marked by t_1 and t_2.

In Fig. 2, we present the ground state phase diagrams obtained for a symmetric mixture, which is characterized by $u_{AA}=u_{BB}=-1$. The topology of those phase diagrams would remain unchanged, however, when $u_{AA}\neq u_{BB}$. The phase diagram shown in Fig. 2(a) corresponds to the situations in which only the pure condensed phases A and B can appear and it occurs whenever $6u_{AB}+u_{\mathrm{as}}\geqslant 3(u_{AA}+u_{BB})$ or $u_{AB}+u_{\mathrm{as}}\geqslant 0.5(u_{AA}+u_{BB})$. The first (second) condition is valid when the inequality (2) is (is not) satisfied. The mixed phase M_1 can be formed for even very small association energy, while the formation of a stable ordered phase M_2 requires that inequality (2) is not fulfilled and that $u_{\mathrm{as}}<0.5(u_{AA}+u_{AB})-u_{AB}$.

Throughout this work, we discuss only the case of $u_{AB}=0$. The interaction parameter $u_{AA}=-1$. Thus, the only interaction parameter, which is allowed to change is u_{as}. For such a model the ground state behavior corresponds to the situation depicted in Fig. 2(a) whenever $u_{\mathrm{as}}\geqslant -1$, and to the situation shown in Fig. 2(b) when $u_{\mathrm{as}}<-1$. In the latter case, the mixed M_2 condensed phase is stable over a certain range of the chemical potentials μ_A and μ_B. In particular, the two triple points t_1 and t_2 marked in Fig. 2(b), are located at

$$t_1:\mu_A=-3.0,\quad \mu_B=-2.0+u_{\mathrm{as}},$$

$$t_2:\mu_A=-2.0+u_{\mathrm{as}},\quad \mu_B=-3.0.$$

All thermodynamic properties and the variables, such as temperature and chemical potentials, are expressed in the units of $|u_{AA}|$: i.e., $T^*=kT/|u_{AA}|$ and $\mu_K^*=\mu_K/|u_{AA}|$, $K=A,B$.

To investigate finite temperature properties of the model, we have applied a standard Monte Carlo method in the

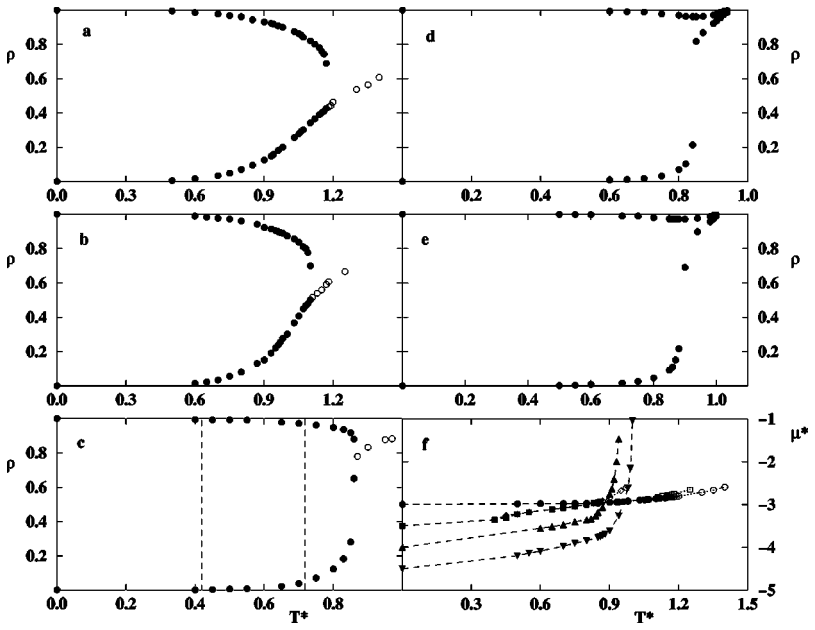

FIG. 3. The phase diagrams in the (T^*,ρ) plane for the systems characterized by different energy of association equal to: (a) 0.0, (b) -1.0, (c) -2.0, (d) -3.0, and (e) -4.0. Filled (open) symbols mark the first-order (continuous) transition points at the coexistence curves. The dashed vertical lines in (c) mark the region over which the gradual demixing is observed. (f) shows the phase diagrams in the (T^*,μ^{ast}) plane for all systems: circles—$u_{\rm as}=0$; squares—$u_{\rm as}=-1$; diamonds—$u_{\rm as}=-2$; triangles up—$u_{\rm as}=-3$ and triangles down—$u_{\rm as}=-4$.

grand canonical ensemble [26] and used the simulation cell of the size $L\times L\times L$, with $L=20$, and the periodic boundary conditions applied in all three space dimensions. An elementary Monte Carlo move, performed at a randomly occupied chosen site consisted in an attempt to either annihilate the particle or to change its identity. When the chosen site was empty, the creation of a randomly chosen particle A or B was attempted. Another elementary move has been an attempt to create or dissociate a dimer. The moves have been accepted following the Metropolis criterion [28].

The number of Monte Carlo moves, per site, used to calculate averages varied between 5×10^6 and 5×10^7 depending on the proximity to the any continuous phase transition point. In general, a larger number of Monte Carlo steps has been used at the temperatures close to the second-order phase transitions. In order to minimize the effects of critical slowing down as well as to minimize the effects of correlations between subsequent configurations, only every nth, with n ranging between 5 and 50, configuration was taken into account during the calculation of averages. A similar number of Monte Carlo steps was used for equilibrating the system.

The basic quantities recorded have been the densities of both species ρ_A and ρ_B, the density of associates $\rho_{\rm as}$, the mole fraction of associated molecules of both components $x_{K,{\rm as}}$, and the average energy (per site) $\langle e\rangle$. Besides, we have calculated the heat capacity, defined as

$$C=\frac{1}{kT^2}[\langle e^2\rangle-\langle e\rangle^2], \tag{3}$$

as well as the susceptibilities associated with the fluctuation of the densities ρ_A, ρ_B, and $\rho_{\rm as}$ are given by

$$\chi_K=\frac{1}{kT}[\langle\rho_K^2\rangle-\langle\rho_K\rangle^2], \quad \text{where } K=A,B,\text{as}. \tag{4}$$

III. RESULTS AND DISCUSSION

Our principal result are the phase diagrams presented in Fig. 3. Figures 3(a) to 3(e) give the T^*-ρ projections, while the Fig. 3(f) shows the T^*-μ^* projections for all the phase diagrams calculated along the path $\mu_A^*=\mu_B^*=\mu^*$, for the systems with different association energy $u_{\rm as}^*$, ranging from 0 to -4.

The phase diagrams obtained for $u_{\rm as}^*=0$ and -1 [cf. Figs. 3(a) and 3(f)] correspond to the situation in which the condensation takes place between the gas phase and a highly demixed liquid, which can be either A or B rich, since the simulation path follows the line of coexistence between those two possible condensed phases $\mu_A^*=\mu_B^*$ (cf. Fig. 2). In these two systems, the mixed, strongly associated ordered phase M_2 can not appear at $T=0$ as well as at finite temperatures. The low temperature region of the first-order condensation transition terminates at the tricritical point, which is the onset of the λ line. Figure 4 shows the isotherms, calculated at the temperatures below and above the tricritical point, which illustrate the changes of the concentration of both components upon condensation. In particular, the continuous demixing transition is quite well seen in the isotherm at $T^*=1.1$. The location of the tricritical point moves toward lower temperatures and higher densities in the system with nonzero association energy. Thus, for $u_{\rm as}^*=0$, the tricritical point is located at $T_{\rm trc}^*\approx1.18$, $\mu_{\rm trc}^*\approx-2.82$ and $\rho_{\rm trc}\approx0.44$, while for $u_{\rm as}=-1.0$ at $T_{\rm trc}^*\approx1.11$, $\mu_{\rm trc}^*\approx-2.82$ and $\rho_{\rm trc}\approx0.515$. Of course, when $u_{\rm as}^*=0$, the association does not take place and in the system with $u_{\rm as}^*=-1.0$ the effects of association are very weak and the fraction of associated molecules at the onset of demixing transition does not exceed 10%. The continuous demixing transition line has been evaluated from the locations of the kinks at the isotherms. These estimations have also been verified by the positions of maxima at the plots of susceptibilities χ_A and χ_B versus μ^* (see Fig. 5). Of course, the heights as well as the positions of

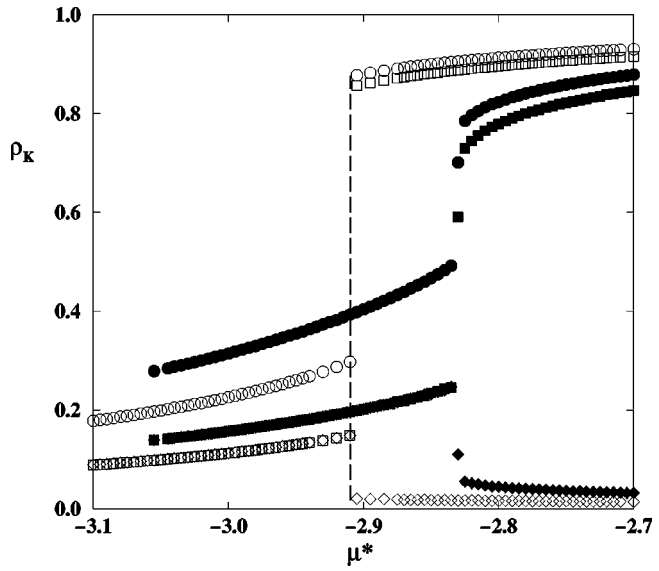

FIG. 4. Isotherms calculated for the system with $u_{as}=-1$ at $T^*=1.0$ (open symbols) and 1.10 (filled symbols). Circles correspond to the total density, while squares and diamonds to the densities of component *A* and *B*, respectively. The vertical dashed line marks the location of the first-order condensation transition.

the susceptibilities maxima are affected by finite size effects [26]. In the thermodynamic limit the height of these peaks should diverge to infinity, as the λ line is a line of critical points. Taking into account that our goal here is rather to provide a qualitative picture of the phase behavior than to give precise estimations of special points on the phase diagrams, we have not attempted to perform any finite size scaling analysis [29].

For the higher energy of association $u^*_{as}=-2$, the topology of the phase diagram looks quite similar [cf. Fig. 3(c)] and the gas-liquid coexistence terminates again at the tricriti-

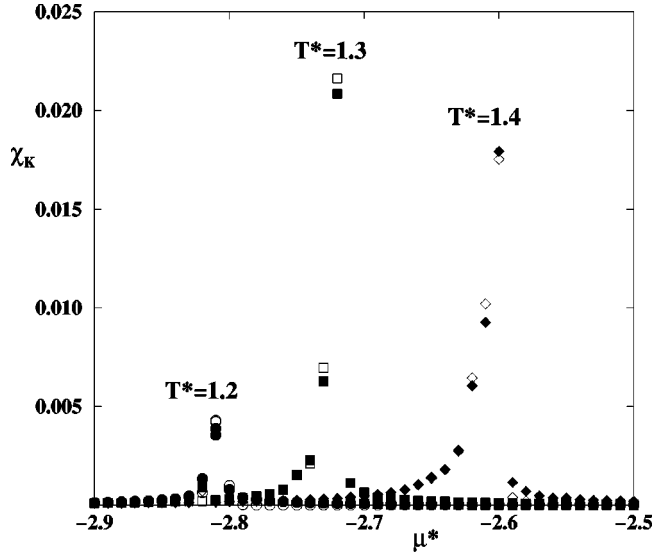

FIG. 5. The plots of χ_A and χ_B against μ^* obtained for the system with $u_{as}=0.0$ at three different temperatures (shown in the figure) above the tricritical point.

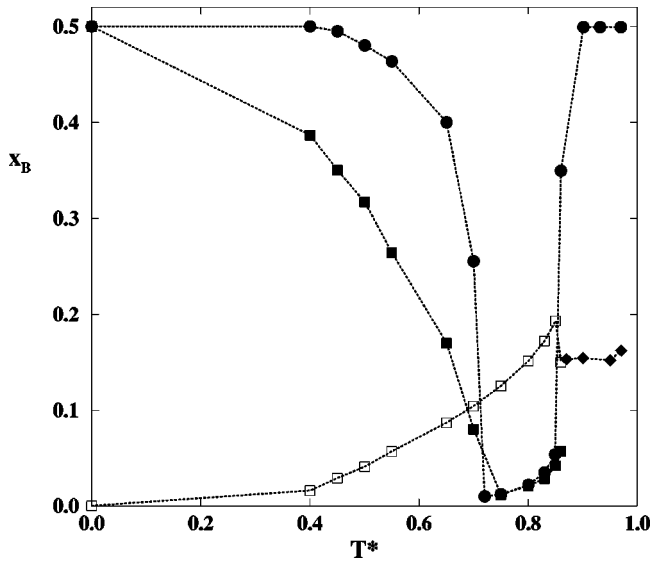

FIG. 6. The mole fraction of the component *B* (filled circles), and the part of the mole fraction of component *B* which forms dimers at both sides of the first-order transition (open squares are for the gas side and filled squares are for the liquid side) as well as along the λ line (filled diamonds), for the system with $u_{as}=-2.0$. The lines are only guides to the eye.

cal point $T_{trc}\approx 0.86$, followed by the λ line. A closer inspection of the system behavior at low temperature reveals, however, that demixing transition occurs already below the tricritical temperature. Figure 6 presents the changes of the mole fraction of component *B* and the fraction of dimers right at the liquid side of the coexistence and at the λ line. Of course, the dilute gas phase has an equimolar composition over the entire range of temperatures, and hence, is not shown in Fig. 6. The composition of the liquid phase gradually changes with increasing temperature and finally the *A* and *B* rich phases separate completely at the temperature of about $T^*_s=0.72$. Also, the mole fraction of associates in the condensed phase decreases with the increase of temperature up to about 0.72. On the other hand, the concentration of associates does not exhibit any pronounced temperature changes along the λ line. Our data suggest that the low temperature demixing is a gradual process rather than a phase transition. At very low temperatures, the condensed phase has the structure corresponding to the M_2 phase.

When $u^*_{as}=-3$ (and -4) the demixing transition does not occur and consequently the topology of the phase diagrams changes [see Figs. 3(d) and 3(e)]. In both cases, the condensation leads to the formation of a quite well ordered M_2 phase and the composition of the fluid, at both sides of the condensation coexistence, corresponds to $x_B=0.5$. In the case of $u_{as}=-3$ the narrow ''neck'' in the phase diagram seems to terminate at the density $\rho=1$, already at the temperature of about $T^*=0.95$. We have calculated the corresponding isotherm over a very wide region of the chemical potential, up to $\mu^*=0.$, and have not found any trace of any phase transition. The increase of the association energy to $u^*_{as}=-4$ causes that the high density part of the coexistence extents to considerably higher temperatures. Figure 7 shows

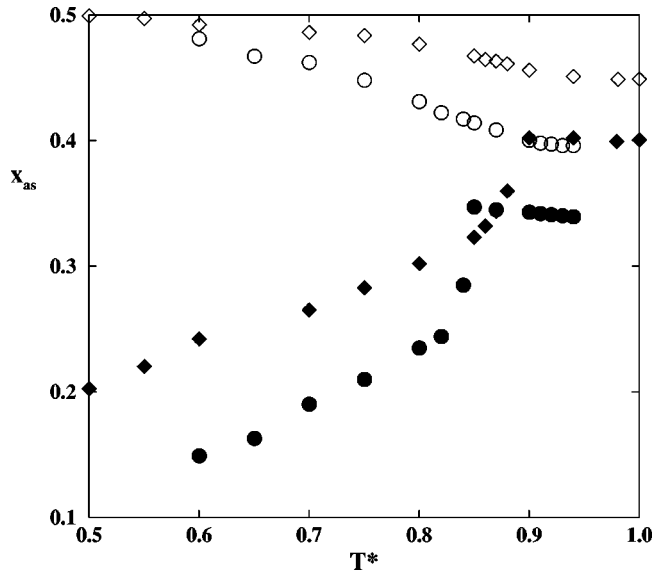

FIG. 7. The part of the mole fraction of component *B* which forms dimers at both sides of the coexistence curve for the systems characterized by $u_{as}=-3$ (circles) and -4 (diamonds). Open symbols are for the liquid side and filled symbols are for the gas side.

the part of the mole fraction of particles *B*, which are involved in associates at both sides of the coexistence curve as a function of temperature for the systems with $u^*_{as}=-3$ and -4. At the side of a dense phase, the degree of association is quite high in both systems. Also, the dilute phase exhibits a rather high degree of association.

The phase diagram depicted in Fig. 8, which corresponds to the system with $u^*_{as}=-3$, has been obtained under quite different conditions. Namely, the chemical potential of one component, say *B*, has been fixed at the value of $\mu^*_B=-4.5$, so that only μ^*_A has been the independent variable. For the chosen value of μ^*_B, the ground state calculations predict that the increase of μ^*_A first leads to the formation of the mixed phase M_2 and then to the condensed pure component *A*. This scenario does hold, but only at the temperatures lower than about 0.54. At higher temperatures, the mixed phase does not develop and the condensed liquid consists of nearly pure component *A*. Note, that the concentration of component *B* above the demixing temperature is practicaly the same at both sides of the coexistence curve [see Fig. 8(a)]. Thus, the system is expected to exhibit the both lower and upper solution critical temperatures, which, of course, cannot be determined from our data. Such an estimation would require to determine phase diagram under different thermodynamic conditions.

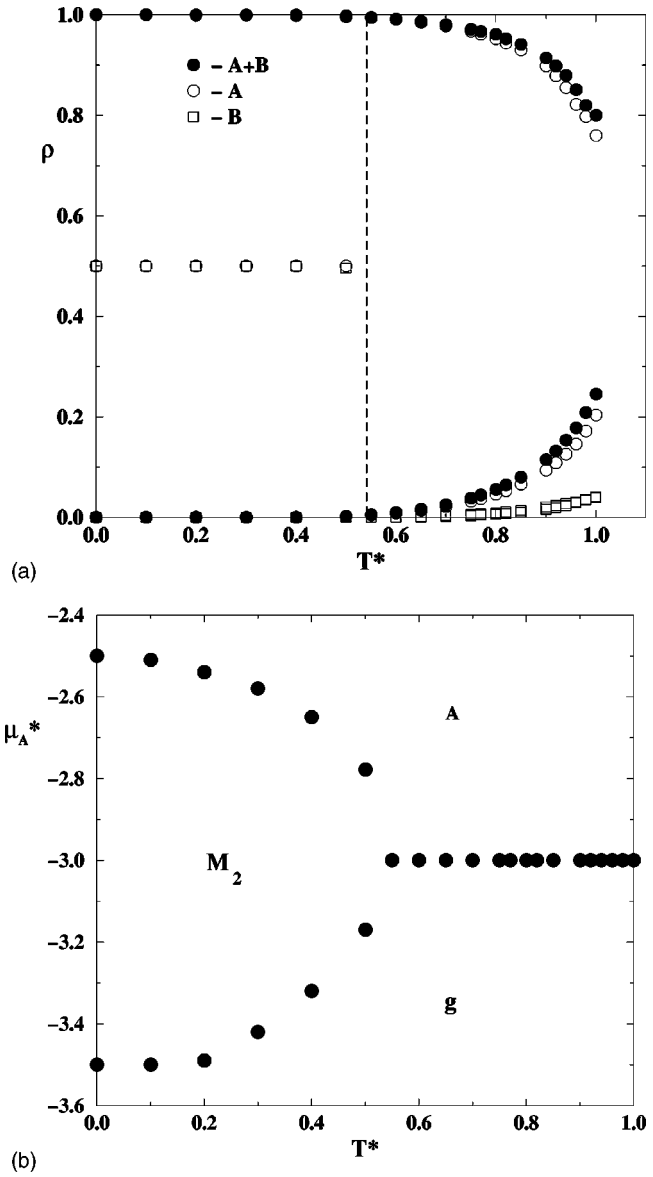

FIG. 8. The phase diagram for the system with $u_{as}=-3$ calculated along the path of the constant chemical potential of component *B*, $\mu^*_B=-4.5$. (a) and (b) show the projections at the (T^*,ρ) and (T^*,μ^{ast}) planes, respectively. In (a), filled circles correspond to the total density, while open squares and diamonds correspond to the densities of component *A* and *B*, respectively.

IV. FINAL REMARKS

The aim of this paper was to elucidate the effects of association on the gas-liquid condensation in binary symmetric mixtures. In particular, we have concentrated on a series of systems with the interaction parameter $u^*_{AB}=0$ and with different energy of association. The nonassociating system exhibits a very strong demixing tendency and its phase diagram belongs to the third class of the classification scheme proposed by Wilding *et al.* [17]. The same holds for the systems with sufficiently low association energy ($u^*_{as}\geqslant -1$), whenever only pure *A* and *B* condensed phases occur in the ground state. When the energy of association becomes higher, the situation is considerably different. At sufficiently low temperatures, the gas-liquid condensation leads to the formation of the ordered mixed phase M_2, while the global phase diagram may look quite similar to the nonassociating case, the first-order condensation ends at the tricritical point followed by the λ line. Thus, there must be a temperature, not exceeding T^*_{trc}, at which the liquid phase becomes demixed. Indeed, the system characterized by $u^*_{as}=-2$ has

been found to undergo the demixing transition well below the tricritical point. The demixing starts already at low temperatures and seems to be a continuous process that terminates at the temperature of about 0.72, whereas the tricritical point for that system is located at $T^*_{\mathrm{trc}} \approx 0.86$. In order to clarify the nature of that demixing transition, one would need to perform suitable Monte Carlo simulation in the Gibbs ensemble rather then in the grand canonical ensemble used here.

For still higher association energies ($u^*_{\mathrm{as}} = -3$ and -4) the demixing transition does not occur at all and the topology of the phase diagram changes and only the first-order transition occurs. The phase diagrams exhibit ''a high temperature neck,'' which corresponds to the transition between highly disordered mixed fluid and the ordered mixed phase M_2. The density difference between these two phases gradually shrinks to zero as the temperature reaches a certain end point value T^*_{end}, whereas the densities of the both coexisting phases go to unity. We have estimated the locations of these end point temperatures for the two systems considered, i.e., with $u^*_{\mathrm{as}} = -3$ and -4. Thus, for $u^*_{\mathrm{as}} = -3$ the end point temperature is equal to $T^*_{\mathrm{end}} \approx 0.95$, and for $u^*_{\mathrm{as}} = -4$ it is equal to $T^*_{\mathrm{end}} \approx 1.02$.

It is expected that other phase diagram topologies would emerge for nonzero values of u^*_{AB}. In particular, in nonassociating symmetric binary mixtures the presence of attractive interaction between unlike particles enhances the tendency toward formation of mixed phases and the appearance of the phase diagrams belonging to the second and first class of Wilding *et al.* [17]. It may be of interest to investigate how the presence of association influences the behavior of such systems. Phase behavior of, even model, associating mixtures is, of course, much more complex and involves various phase transitions between liquid phases [7] that would require future computer simulations in different ensembles and under different thermodynamic conditions.

The above presented results have been obtained as a preliminary step for the investigation of wetting phenomena of associating binary mixtures at walls. A detailed knowledge about the bulk systems is a necessary prerequisite for such a study, which involves calculations of thermodynamic properties close to the bulk condensation. The results of that study will be presented in our next paper.

ACKNOWLEDGMENTS

Financial support of the CONACyT of Mexico under Grant No. 37323-E and the National University of Mexico under Project No. IN101113 is gratefully acknowledged.

[1] K. Marsh and F. Kohler, J. Mol. Liq. **30**, 13 (1985).
[2] J.S. Walker and C.A. Vause, Sci. Am. **256**, 90 (1987).
[3] J.C. Wheeler and G.R. Andersen, J. Chem. Phys. **73**, 5778 (1980).
[4] B.A. Veytsman, J. Phys. Chem. **94**, 8499 (1990).
[5] J.S. Walker and C.A. Vause, J. Chem. Phys. **79**, 2660 (1983).
[6] N.P. Malomuzh and B.A. Veytsman, Phys. Lett. A **136**, 239 (1989).
[7] G. Jackson, Mol. Phys. **72**, 1365 (1991).
[8] A. Robledo, Europhys. Lett., **1**, 303 (1986).
[9] R.E. Goldstein and J.S. Walker, J. Chem. Phys. **78**, 1492 (1983).
[10] M. Kotelyanskii, B. Veytsman, and S.K. Kumar, Phys. Rev. E **58**, R12 (1998).
[11] A. Patrykiejew, O. Pizio, and S. Sokolowski, Phys. Rev. Lett. **83**, 3442 (1999).
[12] P. Bruscolini, A. Pelizzola, and L. Casetti, Phys. Rev. Lett. **88**, 089601 (2002).
[13] L.A. Davies and G. Jackson, and L.F. Rull, Phys. Rev. Lett. **82**, 5285 (1999).
[14] B.A. Veytsman, J. Phys. Chem. B **104**, 11 283 (2000).
[15] J.-C. Lin and P.L. Taylor, Phys. Rev. Lett. **73**, 2863 (1994).
[16] J.-C. Lin and P.L. Taylor, Phys. Rev. E **49**, 2058 (1994).
[17] N.B. Wilding, F. Schmid, and P. Nielaba, Phys. Rev. E **58**, 2201 (1998).
[18] J. S. Rowlinson and F. L. Swinton, *Liquids and Liquid Mixtures* (Butterworth, London, 1982).
[19] L.A. Davies, G. Jackson, and L.F. Rull, Phys. Rev. Lett. **82**, 5285 (1999).
[20] M.S. Wertheim, J. Stat. Phys. **42**, 477 (1986).
[21] G. Jackson, W.G. Chapman, and K.E. Gubbins, Mol. Phys. **65**, 1 (1988).
[22] W.G. Chapman, G. Jackson, and K.E. Gubbins, Mol. Phys. **65**, 1057 (1988).
[23] W.G. Chapman, G. Jackson, K.E. Gubbins, and M. Radosz, Fluid Phase Equilib. **52**, 31 (1989).
[24] P. Bryk, A. Patrykiejew, O. Pizio, and S. Sokołowski, Mol. Phys. **92**, 949 (1997).
[25] M. P. Allen and D. J. Tildesley, *Computer Simulation of Liquids* (Clarendon Press, Oxford, 1987).
[26] D. P. Landau and K. Binder, *A Guide to Monte Carlo Simulation in Statistical Physics* (Cambridge University Press, Cambridge, 2000).
[27] A.Z. Panagiotopoulos, Mol. Phys. **61**, 813 (1987).
[28] A. Sariban and K. Binder, J. Chem. Phys. **86**, 813 (1987).
[29] A.M. Ferrenberg and R.H. Swendsen, Phys. Rev. Lett. **61**, 2635 (1988); **63**, 1195 (1989).